

Intensity correlation measurements in stimulated Raman generation with a multimode laser

L. A. Westling*

*Institute of Optics, University of Rochester, Rochester, New York 14627
and Department of Physics and Astronomy, University of Rochester, Rochester, New York 14627*

M. G. Raymer

Institute of Optics, University of Rochester, Rochester, New York 14627

(Received 29 December 1986)

An experimental and theoretical study of the temporal correlations between the intensities of a broadband pump laser and Stokes light in stimulated Raman generation has been carried out. Direct measurements have been made of the pump laser and Stokes light intensity autocorrelation functions and of the intensity cross-correlation function between the two. Strong cross correlations are found. Nevertheless, the correlations are not perfect; that is, the Stokes intensity does not follow exactly the intensity variations of the laser. Transient effects and quantum fluctuations are shown, by theoretical modeling, to be responsible for the absence of perfect correlations.

I. INTRODUCTION

The statistical properties of the Stokes light in stimulated Raman scattering with broadband pumping have drawn considerable attention in the past and continue to be of interest to experimentalists and theorists alike. The aspect of the previous work which is relevant to the experiments presented here is that pertaining to the correlations between the Stokes and pump laser fields. In 1979, experiments performed by Trutna *et al.*¹ showed that, in the high-gain limit, the gain experienced by the Stokes radiation which builds up from spontaneously scattered light is independent of whether the pump laser is multimode or single model. Similar results were obtained by other research groups.² Stappaerts and co-workers further showed that the multimode, or broadband, gain is decreased when the Stokes and pump laser beams are delayed with respect to each other in the gain medium.³ This gave evidence of the cross correlations between the fields of the laser and Stokes radiation. In recent experiments, Lombardi and Injeyan have used an interferometer to measure the field correlations between Stokes light from a Raman generator and the same light after passing through a Raman amplifier.⁴ The pump laser was time delayed before entering the Raman amplifier. Their results are consistent with the hypothesis that the generated Stokes light from the first Raman cell is correlated with the pump laser, and that is driven into correlation with the delayed pump laser during amplification in the second cell. Zubarev *et al* also carried out experiments (on Brillouin scattering) using an interferometric technique.⁵

Theoretical work has shown that the stimulated Raman generation (as distinct from amplification) process is sensitive to the statistical properties of the pumping laser radiation, in particular to the presence of pump-intensity fluctuations. The broadband laser field has been modeled as phase diffusing,⁶ chaotic,⁷ and pairwise multimode.⁸ When the laser is taken to be phase diffusing the gain of the Stokes wave is found to be independent

of the bandwidth of the laser and hence is independent of phase fluctuations.⁶ It has also been shown that with a laser described by a multimode model in which it is assumed that the Stokes and laser modes interact in a pairwise fashion, the mean Stokes intensity is perfectly correlated with the pump-laser intensity.⁸ By perfect correlation it is meant that the mean Stokes intensity fluctuations follow exactly those of the laser in both shape and relative magnitude. The assumption of the pairwise interaction between Stokes and laser modes is equivalent to assuming that the medium does not respond to any of the laser intensity variations, which are due to mode beating. This means that as far as the medium is concerned, the laser intensity does not fluctuate. In contrast to this is the case where the pump laser field is taken to be chaotic with finite bandwidth.⁷ The gain of the Raman generation process is then found to be very sensitive to the laser bandwidth. This indicates that the gain is sensitive to intensity fluctuations that are not too fast.

The key prediction of the theory applicable to the experiments described here is that the intensity fluctuations of the generated Stokes light are generally correlated with, but not always perfectly correlated with, the laser-intensity fluctuations. The exception occurs when the laser bandwidth is smaller than the Raman linewidth and hence has intensity fluctuations which are slow compared with the relaxation time of the Raman medium. When this occurs the exponential-type gain of the medium responds more to the peaks of the laser-intensity fluctuations than to the valleys. The Stokes intensity then has larger overall fluctuations than does the laser intensity.⁷ The models discussed in the literature represent extremes which can be solved analytically. A more general result can be deduced from these extremes. Whenever the laser intensity varies slowly enough for the medium to follow it, the relative magnitude of the Stokes intensity variations will be greater than those of the pump. Work done by Georges is relevant here.⁹ He addresses the problem of the Raman amplifier pumped

by a chaotic pump field and calculates the amplified Stokes intensity autocorrelation function. He shows that when the laser bandwidth is smaller or comparable to the Raman linewidth the Stokes intensity fluctuations are enhanced over those of the laser. In particular, for the case where the laser linewidth equals the Raman linewidth, and the gain is about 10^6 , there is a predicted enhancement of 10^6 .

The results of studies of the cross correlations between the fields and intensities of the Stokes and laser radiation can be valuable in studies of processes in which fields of widely separated frequencies are necessary. It has been found that in some processes, such as population trapping and double optical resonance, correlations between the fields have a profound effect.¹⁰

Here, we present the results of experiments on Stokes generation which test the theoretical predictions and give the first direct measurement of the cross correlations between the intensities of the laser and the generated Stokes. We have measured the Stokes intensity autocorrelation function and the cross correlation function between the Stokes and laser intensities for two cases: (1) the laser bandwidth Γ_L is larger than the Raman linewidth ($\Gamma_L > \Gamma$) and the laser mode spacing δ is comparable to the Raman linewidth ($\delta \sim \Gamma$), and (2) the laser bandwidth is less than the Raman linewidth ($\Gamma_L < \Gamma$), and the laser mode spacing δ is less than the Raman linewidth ($\delta < \Gamma$). By auto- or cross-correlation function between two intensities $I_A(t)$ and $I_B(t)$ we mean the quantity

$$C_{AB}(T) = \int \langle I_A(t) I_B(t+T) \rangle dt,$$

where the integral is over the duration of the pulse and the brackets indicate an ensemble average over many laser pulses. Such a quantity is convenient to discuss for nonstationary fields and is also readily measured.

The laser used in these experiments was not modeled well by any of the three simple models discussed above. However, as was presented in Ref. 11, the pump laser has been well characterized. This characterization allows us to evaluate the Stokes intensity numerically. We can thus calculate directly the intensity autocorrelation functions for the laser and Stokes intensities as well as their cross-correlation function. Qualitative agreement is found between experiment and theory.

II. EXPERIMENTAL MEASUREMENTS

The experimental setup is shown schematically in Fig. 1. Dye-laser light at 560 nm is Stokes shifted to 730 nm by the $Q(1)$ vibrational transition in hydrogen gas. Hydrogen was chosen because it has high gain, low dispersion, and has been well characterized as a Raman-active medium.¹² Collisional dephasing is the predominant line-broadening mechanism at the pressures used in the experiments (> 10 atm).

The dye laser used as the pump laser for the Raman process has a grazing-incidence-type cavity and its output has a 7-nsec pulse duration. It is pumped by a frequency-doubled, single-longitudinal-mode Nd:YAG laser (where YAG represent yttrium aluminum garnet).

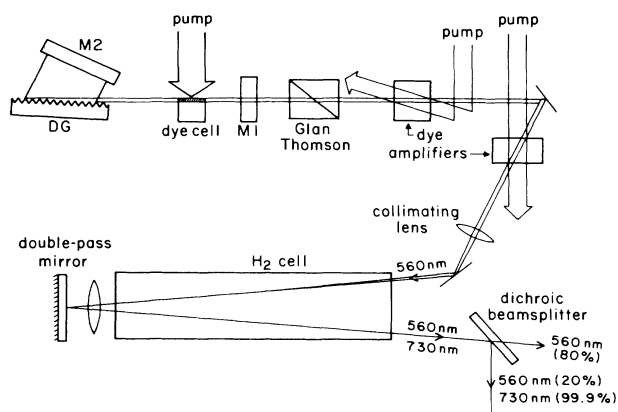


FIG. 1. Schematic of Raman-generation experiment. The light exiting the dye laser first passes through a Glan-Thompson polarizing prism in order to cut out part of the amplified spontaneous emission. After being amplified in two dye amplifiers, the dye laser beam is then collimated to a 400- μm diameter inside the H_2 cell. After the cell a dichroic beamsplitter reflects 99% of the Stokes light (at 730 nm) and 20% of the dye laser (at 560 nm). The collinear beams are then directed to the intensity correlator.

The sensitivity of the dye laser's operation to its cavity configuration was studied in detail and presented in Ref. 11. There we found that our dye laser operates in two limiting configurations: a "correlated-intensity, random-phase" configuration or a "random-intensity, frequency-modulated (FM)-phase-locked" configuration. The intensity autocorrelation function in the "random-intensity, FM-phase-locked" case has a simpler form than that for the "correlated-intensity, random-phase" case. This combined with the fact that it is less difficult to set up the dye laser to operate reliably in the FM-phase-locked configuration led us to choose to use the laser operating in this configuration to perform the Raman experiments.

In order to obtain enough gain to achieve Raman generation, the output of the dye laser was amplified in two dye amplifiers. The final dye laser pulse energy was 2 mJ. The dye used in the oscillator was rhodamine 6G with a concentration of $5 \times 10^{-4} M$ in methanol. The dye amplifiers contained fluorescein dye in methanol plus sodium hydroxide. Fluorescein dye was used in the amplifiers because it has lower absorption at the lasing wavelength of 560 nm than does rhodamine 6G. The concentration of the solution in the first amplifier was $2.5 \times 10^{-4} M$ and the second amplifier concentration was $1.25 \times 10^{-4} M$. Care was taken to amplify the dye-laser light in the linear-gain regime since saturation of the amplifiers would clip off the peaks of the intensity fluctuations. The conversion efficiency in the oscillator amplifier chain was then limited to no greater than about 5%.

In order for the Raman-generation experiments to be modeled well by the one-dimensional theory the laser beam had to be focused throughout the interaction length to achieve a Fresnel number near unity.⁶ This was done by collimating the beam to a diameter of about

400 μm at the center of the H_2 cell, as measured by a linear photodiode array. Since the 100-cm-long cell is double passed, a recollimating lens was needed at the end of the cell where the double-pass mirror was located. The beam diverged slightly at each end of the cell to a diameter of about 500 μm . The appropriate beam diameter can be calculated by setting the Fresnel number F equal to one. Recalling that $F = A / \lambda_S L$, and using an effective cell length $L = 200$ cm, the Stokes wavelength $\lambda_S = 730$ nm, and $A = \pi d^2 / 4$, gives a desired diameter d of about 450 μm , close to that used.

The generated Stokes light travels collinearly with the pump beam. In order to obtain sufficient Stokes intensity to measure its correlation functions, the pump and concomitant Stokes light were double passed through the Raman cell. The light exiting the Raman cell was split by a dichroic beam splitter which reflects 99% of the Stokes light at 730 nm and 20% of the laser light at 560 nm. The reflected beam was then directed into the intensity correlator. This correlator is the same as that described in detail in Ref. 11 and is shown in Fig. 2. Appropriate dichroic filters were placed in each arm of the correlator which passed the proper beam in order to obtain either the pump-intensity autocorrelation function, the Stokes-intensity autocorrelation function or the cross-correlation function between the two intensities. In order to normalize out the shot-to-shot fluctuations of the total energy of the dye-laser pulses the signal from the correlator was divided by the signal from a second correlator with a fixed delay.

The stimulated Raman-generation experiments were performed for two cases. In case 1 the pump laser bandwidth was larger than the Raman linewidth ($\Gamma_L > \Gamma$) and the pump-laser mode spacing δ was comparable to Γ . This case was achieved using a pump laser with a bandwidth $\Gamma_L = 0.10$ cm^{-1} [half width at half maximum (HWHM)] and a mode spacing $\delta = 0.033$ cm^{-1} , and a H_2 pressure of 18.5 atm, which led to a Raman linewidth (HWHM) of $\Gamma = 0.018$ cm^{-1} .

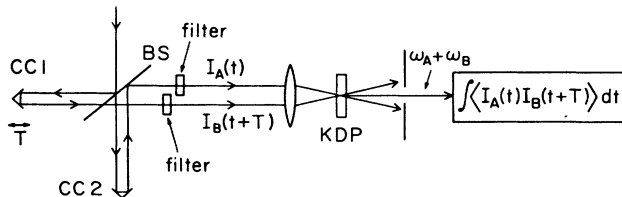


FIG. 2. Intensity correlator. The input light is split into two beams by beam splitter BS and is recombined in the potassium dihydrogen phosphate (KDP) crystal. One of the beams undergoes a variable delay T by means of a movable corner cube CC1. Appropriate filters are placed in each beam in order to obtain the laser- or Stokes-intensity autocorrelation function or the cross-correlation function between the two. The sum-frequency output from the KDP crystal, which is due to the mixing of the two beams, is detected by a photomultiplier tube, the output of which is temporally integrated, giving a direct measurement of the correlation functions $\int \langle I_L(t)I_L(t+T) \rangle dt$, $\int \langle I_S(t)I_S(t+T) \rangle dt$, or $\int \langle I_S(t)I_L(t+T) \rangle dt$, where the brackets $\langle \rangle$ indicate an average over many laser shots.

The correlation measurements for this first case are shown in Figs. 3(a)–3(c). The temporal variations are fairly regular here because the dye laser is operating in an FM-phase-locked configuration.^{11,13} It can be seen, by comparing the shape of the Stokes-intensity autocorrelation function in Fig. 3(b) to the shape of the pump-intensity autocorrelation function in Fig. 3(a), that the variations of the Stokes intensity are similar to those of the pump intensity. Furthermore, the Stokes-laser intensity cross-correlation function shown in Fig. 3(c) shows that there are indeed strong cross correlations between the two intensities. Similarly, the correlation functions from the experimental measurements for case 2, in which $\Gamma_L < \Gamma$ and $\delta < \Gamma$ are shown in Figs. 4(a)–4(c). These were measured using a pump laser with a bandwidth $\Gamma_L = 0.065$ cm^{-1} , a mode spacing $\delta = 0.033$ cm^{-1} , and a H_2 pressure of 100 atm which gives a Raman linewidth of $\Gamma = 0.10$ cm^{-1} .

The depth of modulation of the correlation function $C(T)$ can be defined as $(C_{\text{max}} - C_{\text{min}}) / (C_{\text{max}} + C_{\text{min}})$, where C_{min} and C_{max} are, respectively, the values of $C(T)$ at the minimum closest to $T=0$ and at the subsequent maximum. For case 1, shown in Fig. 3, the depth of modulation is measured to be $0.66(\pm 0.03)$ for the laser autocorrelation function and $0.80(\pm 0.04)$ for the Stokes autocorrelation function. The depth of modula-

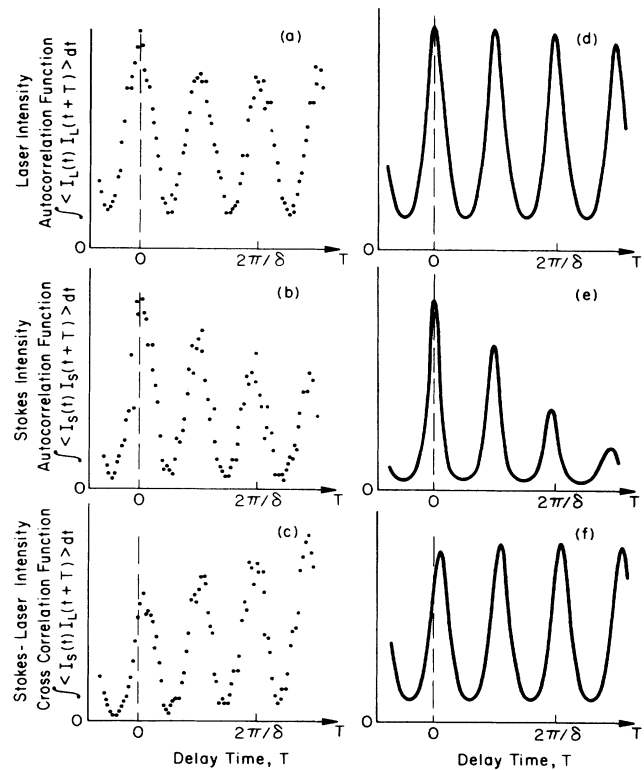


FIG. 3. Intensity correlation functions, experimental (a)–(c) and numerical (d)–(f), for 18.5 atm of H_2 . Raman linewidth (HWHM) $\Gamma = 0.018$ cm^{-1} , laser bandwidth (HWHM) $\Gamma_L = 0.10$ cm^{-1} , laser mode spacing $\delta = 0.033$ cm^{-1} . The time scale is labeled by $2\pi/\delta = 1$ nsec, which is the round-trip time of the laser cavity (δ is in units of rad/sec).

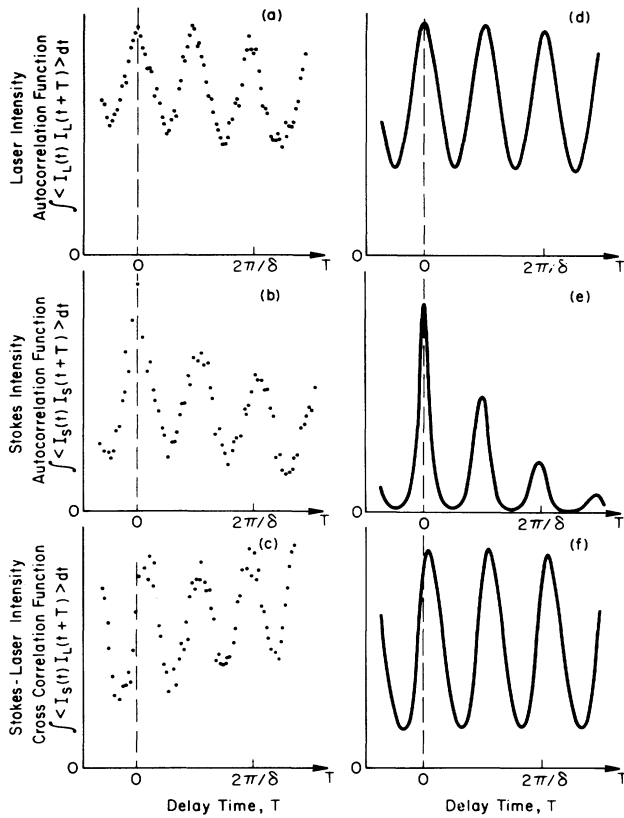


FIG. 4. Intensity correlation functions, experimental (a)–(c) and numerical (d)–(f), for 100 atm of H_2 . Raman linewidth (HWHM) $\Gamma=0.10 \text{ cm}^{-1}$, laser bandwidth (HWHM) $\Gamma_L=0.065 \text{ cm}^{-1}$, laser mode spacing $\delta=0.033 \text{ cm}^{-1}$.

tion of the Stokes autocorrelation function is thus $21(\pm 12)\%$ larger than that of the laser. For case (2), in which the laser bandwidth is less than the Raman linewidth, the depths of modulation of the laser and Stokes autocorrelation functions in Fig. 4 are found to be $0.30(\pm 0.02)$ and $0.49(\pm 0.03)$, respectively. In this case the Stokes depth of modulation is $67(\pm 22)\%$ larger than that of the laser. Hence, the Stokes-intensity fluctuations have been enhanced over those of the laser considerably more in case 2 than in case 1. This is a key result of the present study.

The fact that the Stokes autocorrelation functions decay more rapidly than do the laser autocorrelation functions results from two effects: First, the Stokes pulse envelope is expected to be considerably shorter than the laser pulse so that its intensity decreases significantly 1 ns from the maximum. Second, the Stokes pulse has a coherence time τ_c which is shorter than that of the laser pulse so that Stokes-pulse-shape fluctuations cause the autocorrelation function to decay after a delay time τ_c . In the steady-state regime the coherence time is estimated⁶ to be $\tau_c=(gL)^{1/2}\Gamma^{-1}$, which is equal to 1.7 and 0.30 ns for Figs. 3 and 4, respectively. Indeed, there is some evidence of a narrow spike at $\tau=0$ in Fig. 4(b). Thus, transient pulse shortening and quantum fluctuations of Stokes-pulse shapes are seen to limit the degree of correlation between Stokes and laser intensities.

The shift of the peaks of the cross-correlation functions in Figs. 3(c) and 4(c) indicates that the peaks of the intensity variations of the Stokes pulse are delayed with respect to the corresponding peaks of the laser pulse. The delay of the maximum of the cross-correlation function away from $T=0$ indicates that the peak of the envelope of the Stokes pulse is delayed with respect to the peak of the envelope of the laser pulse. Both of these effects are due to the transient buildup of the Stokes light from the spontaneously scattered light. The degree of transiency can be determined by comparing some relevant time scales. The relation between the laser pulse duration τ_L and the gain response time gL/Γ of the medium determines the degree of transiency.⁶ Here g is the steady-state gain coefficient and L is the transit length through the medium (gain is approximately $\exp[gz]$). In Fig. 3(c), $\tau_L=7 \text{ nsec}$, $1/\Gamma_L=0.053 \text{ nsec}$, $gL=34$, and $\Gamma=3.4 \times 10^9 \text{ rad/sec}$, leading to $gL/\Gamma=10 \text{ nsec}$. Since $\tau_L < gL/\Gamma$ the scattering is transient and there is a delay in the peak of the Stokes pulse and hence a delay in the maximum of the laser-Stokes intensity cross-correlation function. In Fig. 4(c), $\tau_L=7 \text{ nsec}$, $1/\Gamma_L=0.082 \text{ nsec}$, $gL=32$, and $\Gamma=1.9 \times 10^{10} \text{ rad/sec}$, leading to $gL/\Gamma=1.9 \text{ nsec}$, which gives $\tau_L > gL/\Gamma$, indicating steady-state scattering and hence little or no delay in the maximum of the cross-correlation function. In both cases the time scale $1/\Gamma_L$ determined by the laser bandwidth is much less than the gain response time ($1/\Gamma_L \ll gL/\Gamma$), which indicates that the variations of the laser intensity due to mode beating are fast compared with the response of the medium. This causes a delay in the buildup of the individual spikes of the corresponding Stokes-intensity variations. This transiency in the response of the gain to these sharp peaks manifests itself as a shift of the peaks of the cross-correlation function relative to $T=0$. Such a shift has been predicted for a chaotic pump-laser field.¹⁴

III. MODELING OF DATA

A. Modeling of laser

The laser used as the pump in these experiments has previously been statistically characterized by measuring its intensity autocorrelation function¹¹ and the cross correlations between its longitudinal mode intensities.¹⁵ As was mentioned in Sec. II, for the present work, the laser cavity was set up to operate in a configuration in which the mode intensities were random from shot to shot and the mode phases were locked in a FM fashion. For such a laser, the laser field amplitude can be expressed as a sum over the individual mode electric field amplitudes with appropriate phases,

$$E_L(t) = \sum_{n=1}^N A_n(\tau) e^{i\Phi_n} e^{in\delta\tau}, \quad (1)$$

where $\tau=t-z/c$ is the local time, N is the total number of lasing modes, δ is the mode spacing (in rad/sec), and the Φ_n are the individual mode phases. For the FM-locked configuration¹³ the phases are assumed to be constant and given by $\phi_n(n \geq 0)=0$, $\phi_n(n < 0)=0$ (n odd) or

π (n even). The associated laser intensity $|E_L(\tau)|^2$ is given by

$$I_L(\tau) = \bar{I}_L(\tau) + \sum_{k=1}^{N-1} [B_k(\tau)e^{ik\delta\tau} + \text{c.c.}], \quad (2a)$$

where

$$\bar{I}_L(\tau) = \sum_{n=1}^N |A_n(\tau)|^2 \quad (2b)$$

and

$$B_k(\tau) = \sum_{n=1}^{N-k} A_n(\tau)A_{n+k}(\tau)e^{i(\phi_n - \phi_{n+k})}. \quad (2c)$$

The temporal behavior of the intensity of each mode is assumed to be Gaussian in time, with maximum at τ_0 ,

$$|A_n(\tau)|^2 = |A_n(0)|^2 e^{-(\tau - \tau_0)^2 / \sigma^2}, \quad (3)$$

where $\sigma = \tau_L(4 \ln 2)^{-1/2}$, where τ_L is the pump-laser pulse length (FWHM). The frequency spectrum of modes is also assumed to be Gaussian:

$$|A_n(0)|^2 = |A_0|^2 e^{-(n\delta)^2 / \Delta^2}, \quad (4)$$

where $\Delta = \Gamma_L(\ln 2)^{1/2}$ where Γ_L is the HWHM of the laser bandwidth (in rad/sec). Actually the mode intensities $|A_n(0)|^2$ fluctuate from shot to shot by about 20%, but it was found that by making the assumption that they don't fluctuate, good agreement was obtained between experiment and theory for the laser autocorrelation function.¹¹ We will thus make this simplifying assumption in all of the following. Figures 5(a) and 6(a) show $I_L(t)$ calculated in this manner for different bandwidths.

The laser-intensity autocorrelation function as measured in our experiment is defined as

$$C_L(T) = \int \langle I_L(\tau)I_L(\tau+T) \rangle d\tau, \quad (5)$$

where the integration is over the duration of the pulse. For the model calculation of $C_L(T)$ the brackets $\langle \rangle$ are not actually needed since we are assuming that $I_L(t)$ does not change from shot to shot. Examples of the laser-intensity autocorrelation function calculated in this way from Eqs. (2)–(5) for an FM-locked laser, using no free parameters, are shown in Figs. 3(d) and 4(d). It can be seen from a comparison of Fig. 3(d) at $\Gamma_L = 1.9 \times 10^{10}$ rad/sec (0.10 cm^{-1}) with Fig. 4(d) at $\Gamma_L = 1.2 \times 10^{10}$ rad/sec (0.065 cm^{-1}) that the depth of modulation of the intensity autocorrelation function is sensitive to the laser bandwidth. In particular, the depth of the modulation decreases when the laser bandwidth is decreased.

B. Modeling of Stokes generation

Neither of the two experimental cases of Stokes generation studied here is rigorously described by any of the simple theoretical models discussed in the Introduction. For example, the pair-wise multimode model⁸ requires that the laser-mode spacing be much larger than the Raman linewidth, $\delta \gg \Gamma$. In the experiments described here we have either $\delta \sim \Gamma$ or $\delta < \Gamma$. In order for a laser operating with many modes to be fit well by the chaotic

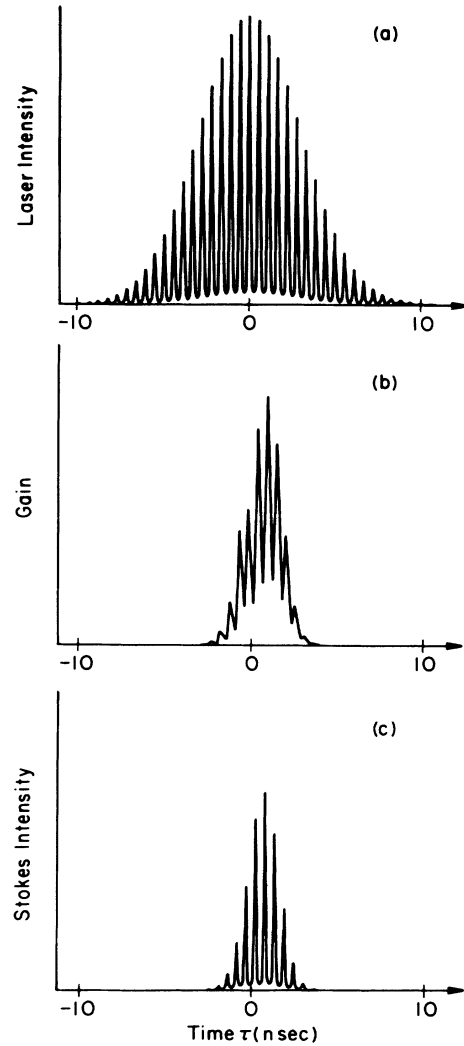


FIG. 5. Results from numerical solution. (a) Intensity of laser $I_L(t)$ operating in FM-locked configuration, from Eq. (2), (b) Stokes gain function $G(t)$ given by Eq. (12), (c) mean Stokes intensity $\langle \hat{I}_S(z,t) \rangle$ [which is equal to the product of (a) and (b)]. Γ , Γ_L , and δ are the same as in Fig. 3, and $gL = 34$.

model⁷ the laser modes must be statistically independent and very closely spaced in frequency ($\delta \ll \Gamma$). The characterization of the output of our dye laser discussed in Ref. 11 revealed that the modes are not independent since either their intensities are correlated or their phases are locked. Hence, in order to compare the experimental results with theoretical predictions the Stokes intensity must be obtained by numerical-integration techniques.

The operator Maxwell-Bloch equations which describe stimulated Raman generation in the low-signal gain regime are⁶

$$\frac{\partial}{\partial z} \hat{E}_S^{(-)}(z,\tau) = -i\kappa_2 E_L(\tau) \hat{Q}^\dagger(z,\tau) \quad (6)$$

and

$$\frac{\partial}{\partial \tau} \hat{Q}^\dagger(z, \tau) = -\Gamma \hat{Q}^\dagger(z, \tau) + i\kappa_1 E_L^*(\tau) \hat{E}_S^{(-)}(z, \tau) + \hat{F}^\dagger(z, \tau). \quad (7)$$

Here $\hat{E}_S^{(-)}(z, \tau)$ is the negative-frequency component of the Stokes field operator, $\hat{Q}^\dagger(z, \tau)$ is the collective molecular vibration operator, $E_L(\tau)$ is the classical pump field, $\tau = t - z/c$ is the local time, Γ and \hat{F}^\dagger describe the collision-induced damping and fluctuations, and the material coefficients κ_1 and κ_2 are given by

$$\kappa_1 = \hbar^{-2} \sum_m d_{3m} d_{m1} \left[\frac{1}{\omega_{m1} - \omega_L} + \frac{1}{\omega_{m1} + \omega_S} \right] \quad (8a)$$

and

$$\kappa_2 = \frac{2\pi N \hbar \omega_S}{c} \kappa_1^*, \quad (8b)$$

where ω_L , ω_S , and ω_{m1} are the laser frequency, Stokes frequency, and difference frequencies between the ground state 1 and the intermediate states m , respectively; d_{nm} are the corresponding dipole matrix elements; and N is the molecular number density. The steady-state gain coefficient is given by $g = 2\kappa_1 \kappa_2 \Gamma^{-1} |E_L|^2$.

The approximate dependence of the fields on only one spatial dimension arises because the interaction volume is taken to be a cylinder with cross-sectional area A and length L , giving a Fresnel number $A/\lambda_S L$ near unity. The following properties of \hat{Q} and \hat{F} are assumed:

$$\langle \hat{Q}^\dagger(z, 0) \hat{Q}(z', 0) \rangle = (AN)^{-1} \delta(z - z'), \quad (9a)$$

$$\langle \hat{F}^\dagger(z, \tau) \hat{F}(z', \tau') \rangle = 2\Gamma (AN)^{-1} \delta(z - z') \delta(\tau - \tau'), \quad (9b)$$

$$\langle \hat{Q}^\dagger(z, 0) \hat{F}(z', \tau') \rangle = \langle \hat{Q}^\dagger(z, 0) \rangle \langle \hat{F}(z', \tau') \rangle = 0. \quad (9c)$$

The brackets $\langle \rangle$ indicate a quantum expectation value taken in the initial state with all molecules in their ground states and the Stokes field in an arbitrary state. Equation (9a) describes the initial quantum noise in the vibrational coordination \hat{Q} , which is responsible for initiating the Stokes generation. Equation (9b) describes the collisional fluctuations.

In the generator case, where no input Stokes wave is present, Eqs. (6) and (7) must be solved in space and time, due to the presence of the fluctuations \hat{F} , which cause \hat{Q} and $\hat{E}_S^{(-)}$ to vary randomly on a time scale Γ^{-1} . These equations have been solved exactly using Laplace

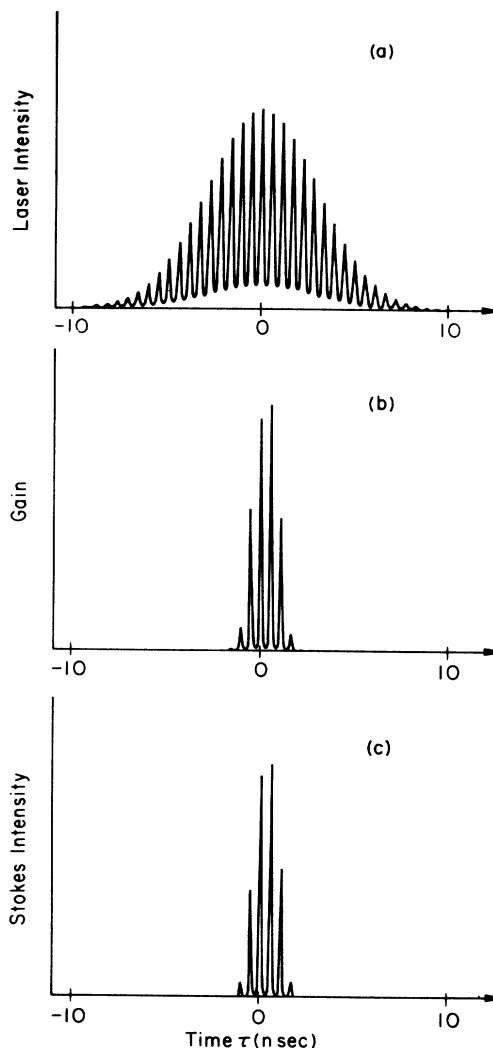


FIG. 6. Results from numerical solution. (a) Intensity of laser $I_L(t)$ operating in FM-locked configuration, (b) Stokes gain $G(t)$, (c) mean Stokes intensity $\langle \hat{I}_S(z, t) \rangle$ [which is equal to the product of (a) and (b)]. Γ , Γ_L , and δ are the same as in Fig. 4, and $gL = 32$.

transform techniques to give for the Stokes field⁶

$$\hat{E}_S^{(-)}(z, \tau) = \hat{E}_S^{(-)}(0, \tau) + \hat{\xi}(z, \tau) E_L(\tau), \quad (10a)$$

where the operator $\hat{\xi}(z, \tau)$ is given by

$$\begin{aligned} \hat{\xi}(z, \tau) = & (\kappa_1 \kappa_2 z)^{1/2} \int_0^\tau d\tau' \left[e^{-\Gamma(\tau-\tau')} E_L^*(\tau') \hat{E}_S^{(-)}(0, \tau') \frac{I_1(\{4\kappa_1 \kappa_2 z [p(\tau) - p(\tau')]\}^{1/2})}{[p(\tau) - p(\tau')]^{1/2}} \right] \\ & - i\kappa_2 e^{-\Gamma\tau} \int_0^z dz' \hat{Q}^\dagger(z', 0) I_0([4\kappa_1 \kappa_2 (z - z') p(\tau)]^{1/2}) \\ & - i\kappa_2 \int_0^\tau d\tau' \int_0^z dz' e^{-\Gamma(\tau-\tau')} \hat{F}^\dagger(z', \tau') I_0(\{4\kappa_1 \kappa_2 (z - z') [p(\tau) - p(\tau')]\}^{1/2}), \end{aligned} \quad (10b)$$

where the $I_n(x)$ are modified Bessel functions and

$$p(\tau) = \int_0^\tau |E_L(\tau'')|^2 d\tau'' \quad (10c)$$

is the power of the laser field integrated up to time τ ,

In Eq. (10), $\hat{E}_S^{(-)}(0, \tau)$ is the free-field Stokes operator at the input to the medium. In the quantum generator case the Stokes field is initially in the vacuum state, which gives zero when operated on by the free-field operator $\hat{E}_S^{(+)}(0, \tau)$. Thus terms containing $\hat{E}_S^{(-)}(0, \tau)$ give no contribution to the Stokes intensity (in normal ordering). The Stokes-intensity operator is

$$\hat{I}_S(z, \tau) = \hat{E}_S^{(-)}(z, \tau) \hat{E}_S^{(+)}(z, \tau). \quad (11)$$

Hence the Stokes intensity averaged over a (quantum) ensemble of Stokes pulses is given, for a particular form of $I_L(\tau)$, by

$$\langle \hat{I}_S(z, \tau) \rangle = G(\tau) I_L(\tau), \quad (12a)$$

where

$$G(\tau) \equiv \langle \hat{g}(z, \tau) \hat{g}^\dagger(z, \tau) \rangle \quad (12b)$$

is called the Stokes "gain function" because it contains the medium's response to the laser and determines the resulting shape of the Stokes intensity function. One can think of the laser intensity $I_L(\tau)$ as "scattering off" of the gain function $G(\tau)$ to produce $\langle \hat{I}_S(\tau) \rangle$. Using Eqs. (9) and (10) the gain function is found to be

$$G(\tau) = \frac{|\kappa_2|^2}{AN} \left[e^{-2\Gamma\tau} \int_0^z dz' I_0^2([4\kappa_1\kappa_2(z-z')p(\tau)]^{1/2}) \right. \\ \left. + 2\Gamma \int_0^\tau d\tau' \int_0^z dz' e^{-2\Gamma(\tau-\tau')} I_0^2(\{4\kappa_1\kappa_2(z-z')[p(\tau)-p(\tau')]\}^{1/2}) \right]. \quad (12c)$$

The Stokes-intensity autocorrelation function $C_S(T)$ can be calculated from

$$C_S(T) = \int \langle \langle \hat{I}_S(z, \tau) \hat{I}_S(z, \tau+T) \rangle \rangle d\tau, \quad (13)$$

where the double bracket $\langle \langle \rangle \rangle$ is a quantum expectation value and a classical average over laser fluctuations. This result holds for any laser field. If we make the assumption that the laser-intensity temporal structure does no change from shot to shot, as is approximately the case for our FM-phase-locked laser, then we can drop the average over laser fluctuations and replace the double bracket by a single bracket. In further simplifying Eq. (13) it is useful to note that the Stokes field can be treated as a classical, complex Gaussian random process.¹⁶ With this information Eq. (13) can be rewritten with the help of the moment theorem for such a process U_i ,

$$\langle U_1^* U_2^* U_3 U_4 \rangle = \langle U_1^* U_3 \rangle \langle U_2^* U_4 \rangle + \langle U_1^* U_4 \rangle \langle U_2^* U_3 \rangle, \quad (14)$$

to give

$$C_S(T) = \int [\langle \hat{I}_S(z, \tau) \rangle \langle \hat{I}_S(z, \tau+T) \rangle \\ + |\langle \hat{E}_S^{(-)}(z, \tau) \hat{E}_S^{(+)}(z, \tau+T) \rangle|^2] d\tau, \quad (15)$$

where $\langle \hat{I}_S(z, \tau) \rangle$ is given by Eq. (12).

The second term in Eq. (15) is just the square modulus of the Stokes-field autocorrelation function, which has

been calculated to be¹⁷

$$\langle \hat{E}_S^{(-)}(z, \tau_1) \hat{E}_S^{(+)}(z, \tau_2) \rangle \\ = \frac{2|\kappa_2|^2 z E_L(\tau_1) E_L^*(\tau_2)}{AN q(\tau_1, \tau_2)} e^{-\Gamma(\tau_1+\tau_2)} \\ \times \left[f(\tau_1, \tau_2) + 2\Gamma \int_0^s e^{2\Gamma t'} g(t') dt' \right], \quad (16a)$$

where s is the lesser of τ_1 and τ_2 and

$$q(\tau_a, \tau_b) = 4\kappa_1\kappa_2 z \int_{\tau_b}^{\tau_a} |E_L(t')|^2 dt', \\ f(\tau_1, \tau_2) = [q(\tau_1, 0)]^{1/2} I_1([q(\tau_1, 0)]^{1/2}) \\ \times I_0([q(\tau_2, 0)]^{1/2}) - (\tau_1 \leftrightarrow \tau_2), \quad (16b)$$

and

$$g(t') = [q(\tau_1, t')]^{1/2} I_1([q(\tau_1, t')]^{1/2}) \\ \times I_0([q(\tau_2, t')]^{1/2}) - (\tau_1 \leftrightarrow \tau_2). \quad (16c)$$

The laser-Stokes intensity cross correlation function $C_{LS}(T)$ can be calculated from

$$C_{LS}(T) = \int \langle \langle \hat{I}_S(\tau) I_L(\tau+T) \rangle \rangle d\tau. \quad (17)$$

If it is again assumed that the laser intensity does not fluctuate Eq. (17) can be written as

$$C_{LS}(T) = \int \langle \hat{I}_S(z, \tau) \rangle I_L(\tau+T) d\tau. \quad (18)$$

C. Results of modeling

In order to evaluate Eqs. (15) and (18) for comparison with the experimentally measured correlation functions,

Eqs. (12) and (16) were evaluated numerically including the properties of the multimode pump laser, described in Eqs. (1)–(4). To simplify the evaluation of the gain function $G(\tau)$ via Eq. (12c), we chose $\Gamma\tau_0 \gg 1$, where τ_0 is seen in Eq. (3) to be the time of the laser-pulse maximum. The value of τ_0 is arbitrary, but this choice simplifies Eq. (12c) by causing the first of the two terms there to drop out.

In order to model the Stokes generation the gain coefficient gL must be estimated, where $g = g_0 I_L$ and $L = 200$ cm. Using the published¹² value $g_0 = 2.5 \times 10^{-9}$ cm/W and the estimated value of the laser intensity I_L gives a value of gL that is about three times too large, leading to a predicted Stokes-generation intensity that is much too large. Since the laser beam was not well characterized spatially and probably had a lot of power in the wings, we adjusted the peak value of I_L down to give $gL = 34$ or 32 for the 18.5- or 100-atm data, respectively. This gave a calculated conversion efficiency of several percent, close to that seen experimentally.

Figures 5 and 6 show the resulting theoretical plots of $I_L(\tau)$, $G(\tau)$, and $\langle \hat{I}_S(\tau) \rangle$. Examination of these plots reveals, qualitatively, the effect of changing the medium response time with respect to the time scale of the pump-intensity variations. The plots of the gain function $G(\tau)$ in Figs. 5(b) and 6(b) are particularly telling. For the case in Fig. 5(b) where $\Gamma_L > \Gamma$ and $\delta \sim \Gamma$, the medium response is slow and the gain function $G(\tau)$ appears smoother than that in Fig. 6(b) where the medium response is faster or comparable to the laser-intensity variations ($\Gamma_L \sim \Gamma$, $\delta \gg \Gamma$). It should also be noted that the Stokes-pulse envelope is considerably shorter than the laser-pulse envelope, as anticipated in connection with Figs. 3 and 4.

In order to model the correlation data shown in Figs. 3 and 4 the correlation functions $C_L(T)$, $C_S(\tau)$, and $C_{LS}(\tau)$ were calculated using Eq. (16) and the pump and Stokes intensities shown in Figs. 5 and 6. The results of the numerical calculations are shown in Figs. 3(d)–(f) and 4(d)–(f). In Fig. 3, the agreement between the data and the modeling is reasonably good, although the theoretical Stokes-intensity autocorrelation function decays somewhat faster than the experimental one and has a sharper central peak.

The delay of the maximum of the cross-correlation function in Figs. 3(c) and 3(f) from $T=0$ can be understood in more detail by considering the limiting form for the high-gain transient buildup of the Stokes intensity,¹⁷

$$\langle \hat{I}_S(z, \tau) \rangle \simeq \frac{|E_L(\tau)|^2}{8\pi p(\tau)} e^{[16\kappa_1 \kappa_2 L p(\tau)]^{1/2}}, \quad (19a)$$

where

$$p(\tau) = \int_{-\infty}^{\tau} |E_L(\tau')|^2 d\tau'. \quad (19b)$$

This equation shows more simply than Eq. (12) how the Stokes intensity depends on the temporal properties of the pump intensity. The effect of this dependence for the pump used in the experiments can be seen by considering the modeled pump and Stokes intensities in Fig. 5. There it can be seen that the maximum of the Stokes-

intensity envelope is delayed with respect to the maximum of the laser-pulse envelope. Careful inspection reveals that this delay appears not only as a shift of the entire Stokes envelope but also as a shift of the individual spikes of the Stokes-intensity variation. The shift of the Stokes-pulse envelope translates into the delay of the maximum of the cross-correlation function from $T=0$ to approximately $2\pi/\delta$ in Fig. 3(f). The delay of the individual spikes of the Stokes intensity translates into the shifts of the individual peaks of the cross-correlation function relative to $T=0$. The modeled cross-correlation function fits the shifts of the intensity spikes but not the delay of the maximum due to the Stokes-pulse delay. It appears that the Stokes pulse was delayed more, and hence was more transient, in the experiment than the experimental parameters and theory would predict. This increased delay can be achieved in the modeling by either increasing the gain coefficient gL by a factor of about 2 or by decreasing the Raman linewidth by a factor of about 3.5. Increasing gL by a factor of 2 results in an unrealistic value of $\sim 10^{36}$ for the total number of photons N_S . Decreasing the Raman linewidth by a factor of 3.5, for example, gives a realistic value for N_S ($\sim 10^{16}$) and will help fit the delay of the maximum of the cross-correlation function in Fig. 3(f). It does not, however, fit the shift of the peaks.

The modeling of the correlation data for the case where $\Gamma_L \sim \Gamma$ and $\delta \ll \Gamma$ is shown in Figs. 4(d)–4(f). We again see the shift of the cross-correlation peaks due to the delay of the Stokes-intensity spikes described above. Inspection of Fig. 6 reveals that the maximum of the Stokes pulse is not delayed much with respect to the maximum of the laser pulse so the maximum of the cross-correlation function is found near $T=0$ in Fig. 4(f).

The depth of modulation of the theoretical correlation functions can be calculated using the algorithm used for the experimental correlation functions. For case 1, the depth of modulation of the functions in Figs. 3(d) and 3(e) are 0.75 and 0.86 for the laser and Stokes autocorrelation functions, respectively. These results yield a 15% enhancement of the depth of modulation of the Stokes autocorrelation function over that of the laser, which is in reasonable agreement with the 21(± 12)% enhancement obtained from the data. Similarly, the modulation enhancement for case 2 can be calculated from the depth of modulation of the laser and Stokes autocorrelation functions in Figs. 4(d) and 4(e). These values are found to be 0.44 and 0.94, respectively, yielding a 114% enhancement. This is not in very good agreement with the 67(± 22)% enhancement calculated from the data in Figs. 4(a) and 4(b). This disagreement can be attributed to the 33% difference in the depths of modulation of the measured and modeled laser-intensity autocorrelation functions in Figs. 4(a) and 4(d). Note that the autocorrelation function of the laser intensity shown in Fig. 4(d) was calculated using *no* adjustable parameters. Judicious adjustment of the laser bandwidth within experimental error could have been done to fit the data better. Unfortunately, the complexity of the calculation, and hence the required computer time, prevented us from re-

peating the calculation of the Stokes-intensity autocorrelation function with the laser bandwidth as an adjustable parameter.

Thus we see that the simple modeling with only the gain coefficient as a free parameter does not completely predict the behavior of this complex system, but that overall there is good qualitative agreement between the data and the model. Other possible causes for the discrepancies between the model and the data are the following. In using the model for the laser intensity given by Eq. (2) we assumed that the laser-mode intensities are constant from shot to shot. Actually the mode intensities fluctuated by about 20%.¹¹ Another possible source for the discrepancy is that the theory applies strictly to an unsaturated Raman process, i.e., no pump-laser depletion or population transfer is accounted for. In order to obtain experimentally a large enough average Stokes energy to measure correlation functions it was necessary to produce large Stokes pulses, some of which were possibly saturating the gain. The presence of these larger Stokes pulses is due to the fact that the Stokes energy exhibits macroscopic quantum fluctuations, which means that the total Stokes energy can fluctuate by 100% or more from its mean value.¹⁸ The effect of the saturated pulses on the correlation data is not certain.

The apparent background slope of the cross-correlation function in Fig. 4(c) is an experimental artifact and has two probably causes: a slight misalignment of the correlator or a decrease of the success rate of single-mode Nd:YAG laser pulses which pump the dye laser. The correlator is very sensitive to misalignment, especially when the two beams are of different frequencies and slightly different spatial quality. This could lead to slope in the correlation function as the correlator was scanned. The Nd:YAG pulses are monitored with a fast photodiode. The Nd:YAG operates in either one or two longitudinal modes on each shot. If it operates in two modes the fast beating on the temporal profile is observed and the data are rejected for that shot. Hence if a number of double-mode shots occur in a short time fewer data points will be collected and the intensity correlation function will have a slightly worse signal-to-noise ratio at that time.

IV. CONCLUSIONS

We have presented the results of an experimental study of the correlations between the pump laser and Stokes intensities in stimulated Raman generation. It has been shown, as the theory in the literature predicted,

that the magnitude of the Stokes-intensity variations is a sensitive function of the time scale of the laser-intensity variations relative to the response time of the Raman-gain process. This was accomplished by measuring the Stokes-intensity autocorrelation function and the cross-correlation function between the Stokes and laser intensities and comparing those functions with the laser-intensity autocorrelation function.

In this manner we experimentally verified the following two predictions. First, when the intensity variations are fast compared with the response time of the medium, the medium acts largely to average over them. This means that the Stokes-intensity variations nearly follow those of the laser. In the other extreme, when the laser-intensity variations are slow enough for the medium to respond to them, the exponential-type gain of the medium amplifies the Stokes light at the peaks of the laser-intensity variations more than at the valleys, leading to an increase in the overall relative Stokes-intensity variations. Second, when the Stokes scattering is transient ($\tau_L < gL/\Gamma$) the peaks and position of the maximum in the laser-Stokes intensity cross-correlation function are delayed from zero. Also, we found that transient pulse shortening and quantum fluctuations limit the degree of correlation between Stokes and laser intensities.

The measured correlation functions were modeled by numerically calculating the Stokes intensity with the assumption that the laser intensity was well described as that from a laser which is operating with modes which have constant intensities and FM-locked phases. Good qualitative agreement was found between the data and the modeling.

The results of this study thus show that one cannot assume *a priori* that the scattered radiation in the stimulated Raman process has its field and intensity perfectly correlated with those of the laser. This is especially important in processes requiring more than one input beam, many of which have been shown to be sensitive to the cross correlations between the input fields and/or intensities.⁹ If stimulated Raman scattering were used to generate coherent light for use in studies of this type, the degree of cross correlation between the Stokes and laser intensities would have a profound effect.

ACKNOWLEDGMENTS

This work was supported by the U.S. Department of Energy, Basic Energy Sciences, Chemical Sciences Division. We would like to thank J. H. Eberly for his continuing interest and helpful discussions throughout the course of this research.

*Present address: Joint Institute for Laboratory Astrophysics, University of Colorado, Boulder, CO 30309.

¹W. R. Trutna, Y. K. Park, and R. L. Byer, IEEE J. Quantum Electron. **QE-15**, 648 (1979).

²For example, see S. A. Akhmanov, Yu. E. D'yakov, and L. I. Pavlov, Zh. Eksp. Teor. Fiz. **66**, 520 (1974) [Sov. Phys.—JETP **39**, 249 (1974)]; G. P. Dzhotyan, Yu. E. D'yakov, I. G. Zubarev, A. B. Mironov, and S. I. Mikhailov, *ibid.* **73**, 822

(1977)] [*ibid.* **46**, 431 (1977)] and Kvantovaya Elektron. (Moscow) **4**, 1377 (1977) [Sov. J. Quantum Electron. **7**, 783 (1977)].

³E. A. Stappaerts, W. H. Long, Jr., and H. Komine, Opt. Lett. **5**, 4 (1980).

⁴G. G. Lombardi and H. Injeyan, J. Opt. Soc. Am. B **3**, 1461 (1986).

⁵I. Zubarev, A. Mironov, S. Mikhailov, and A. Okulov, Zh.

- Eksp. Teor. Fiz. **84**, 466 (1983) [Sov. Phys.—JETP **57**, 270 (1983)].
- ⁶M. G. Raymer and J. Mostowski, Phys. Rev. A **24**, 1980 (1981).
- ⁷M. Trippenbach, K. Rzazewski, and M. G. Raymer, J. Opt. Soc. Am. B **1**, 671 (1984).
- ⁸M. G. Raymer and L. A. Westling, J. Opt. Soc. Am. B **2**, 1417 (1985).
- ⁹A. T. Georges, Opt. Commun. **41**, 61 (1982).
- ¹⁰B. J. Dalton and P. L. Knight, J. Phys. B **15**, 3997 (1982); and B. J. Dalton, R. McDuff, and P. L. Knight, Opt. Acta **32**, 61 (1985); T. A. B. Kennedy and S. Swain, J. Phys. B **17**, L389 (1984); and S. Swain, J. Opt. Soc. Am. B **2**, 1666 (1985).
- ¹¹L. A. Westling and M. G. Raymer, J. Opt. Soc. Am. B **3**, 911 (1986).
- ¹²E. E. Hagenlocker, R. W. Minck, and W. G. Rado, Phys. Rev. **154**, 226 (1967); Ford Motor Co. Tech. Report SL66-24, 1966 (unpublished); W. K. Bischel and M. J. Dyer, Phys. Rev. A **33**, 3113 (1986); and J. Opt. Soc. Am. B **3**, 677 (1986).
- ¹³A. E. Siegman, *Lasers* (University Science Books, Mill Valley, 1986), p. 1051.
- ¹⁴M. Trippenbach and Cao Long Van, J. Opt. Soc. Am. B **3**, 879 (1986).
- ¹⁵L. A. Westling, M. G. Raymer, and J. J. Snyder, J. Opt. Soc. Am. B **1**, 150 (1984).
- ¹⁶R. Glauber and F. Haake, Phys. Lett. **68A**, 29 (1978); M. G. Raymer, K. Rzazewski, and J. Mostowski, Opt. Lett. **7**, 71 (1982); J. Mostowski and B. Sobolewska, Phys. Rev. A **30**, 610 (1984); and I. A. Walmsley, Ph.D. Thesis, University of Rochester, 1986 (unpublished).
- ¹⁷M. G. Raymer, I. A. Walmsley, J. Mostowski, and B. Sobolewska, Phys. Rev. A **32**, 332 (1985).
- ¹⁸I. A. Walmsley and M. G. Raymer, Phys. Rev. A **33**, 382 (1986).